This is the accepted manuscript made available via CHORUS. The article has been published as:

Antimony bonding in Ge-Sb-Te phase change materials

David C. Bobela, P. Craig Taylor, Phillip Kuhns, Arneil Reyes, and Arthur Edwards

Phys. Rev. B **83**, 033201 — Published 13 January 2011

DOI: 10.1103/PhysRevB.83.033201

Antimony bonding in Ge-Sb-Te phase change materials

David C. Bobela*
Department of Physics, University of Utah, Salt Lake City, Utah USA

P. Craig Taylor
Department of Physics, Colorado School of Mines, Golden, Colorado USA

Phillip Kuhns, Arneil Reyes
National High Magnetic Field Laboratory, Tallahassee, Florida USA

Arthur Edwards
Air Force Research Laboratory, RVSE, Kirtland Air Force Base, New Mexico USA 87117-5776

Abstract

The amorphous phase in some technologically important Ge-Sb-Te systems is still not well understood despite many models that exist to explain it. Using nuclear magnetic resonance, we demonstrate that Sb bonding in these systems follow the "*8-n"* rule for chemical bonding in amorphous solids. We find that the Sb atoms preferentially bond to three atoms in a pyramidal configuration analogous to the sites occurring in Sb-S or Sb-Se systems. The data we present should be used as a guide for structural modeling of the amorphous phase.

PACS numbers: 61.43.Dq , 61.05.Qr

*corresponding author, now at National Renewable Energy Laboratory, Golden, Co 80401

I. Introduction

Many compounds of germanium, antimony, and tellurium undergo rapid phase-transformations between polycrystalline and amorphous states under the influence of optical or electrical excitation. These transformations are accompanied by significant changes in reflectivity and very large changes in conductivity. The use of these phase change materials (PCM's) as an active element of many electronic applications is rapidly coming to fruition. Currently, most rewriteable digital versatile disks (DVD-RW's) rely on $Ge_2Sb_2Te_5$. Non-volatile, electrically switched PCM-based memories, which exploit the large conductivity change, are also under active investigation and development. Although these PCM's have been studied for many years [1], details of the phase-change mechanism are controversial, mostly because of the difficulty in accessing structural information on the nanometer scale. There is no detailed understanding of the local (nearest neighbor) and intermediate structural order in the amorphous phase. In fact, the local structure of the amorphous phase of Ge-Sb-Te phase-change-memory alloys has been the subject of considerable controversy. From extended x-ray absorption fine structure (EXAFS) experiments, Kolobov *et al.* first suggested that the local nearest neighbor coordination of Ge in $Ge_2Sb_2Te_5$, the composition used in many DVD-RW applications, changed from six in both of the crystalline phases to four in the amorphous phase but that the Sb and Te coordinations remained essentially the same (six) in all phases [2]. Baker, *et al.*, and more recently Jovaria *et al.* have reported EXAFS data on as-deposited, amorphous material [3,4]. Here, it is clear that the coordination changes dramatically around all species. The best fit to the data was consistent with the *8-N* rule, where coordination numbers around all Ge, Te, and Sb atoms are four, two, and three, respectively. Hegedüs and Elliot have observed

structures that are either suggestive of, if not consistent with, the *8-N* model in an extensive investigation of the kinetics of a complete phase cycle for a supercell of $Ge_2Sb_2Te_5$ [5].

While EXAFS has dominated the experimental literature for the GST compounds, nuclear magnetic resonance (NMR) has been used with great success to determine local bonding structures in many materials, including As_2Se_3, As_2S_3, and Ge-As-Se compounds (see for instance, Refs [6-8] and references therein). In a preliminary study, Bobela and Taylor have exploited the ^{125}Te NMR chemical shift to study some of the GST alloys [9]. They found that the ^{125}Te spectrum in amorphous $Ge_2Sb_2Te_5$, consists of two Gaussian-like features, whereas the spectrum for the crystalline counterpart consists of a single Gaussian-like feature, shifted in frequency spaced. This simple observation was the first evidence that the tellurium bonding depends on the system's phase. Although these NMR data are insufficient to provide the tellurium bonding structures, Bobela and Taylor found that each of components in the amorphous $Ge_2Sb_2Te_5$ spectrum can be well explained by the spectra they measured for amorphous $Ge_2Sb_2Te_4$ and $Ge_2Sb_2Te_7$ [9]. In fact, the $Ge_2Sb_2Te_7$ ^{125}Te spectrum resembles the spectrum measured in amorphous tellurium, where it is known that tellurium bonds to two other tellurium atoms, in accordance with the *8-N* rule. Bobela and Taylor therefore concluded that the predominant tellurium bonding giving rise to the amorphous $Ge_2Sb_2Te_4$ (predominant bonding configuration unknown) and $Ge_2Sb_2Te_7$ spectra (primarily two-fold coordinated tellurium) are *both* present in amorphous $Ge_2Sb_2Te_5$. The Kolobov model for the amorphous phase cannot account for this experimental observation.

In this report, we demonstrate that the *8-N* principle holds also for the Sb nucleus in $Ge_2Sb_2Te_4$, $Ge_2Sb_2Te_5$, and $Ge_2Sb_2Te_7$. Here, we exploit NMR to probe the interaction between the nuclear quadrupole moment of the ^{121}Sb nucleus (~ 50% naturally abundant) and the electric

field gradient (EFG) created by the surrounding electric charge [10]. At sufficiently high applied magnetic fields, the NMR spectra directly reflect the angular averaging of the quadrupolar interaction, whose magnitude and symmetry can be modeled using standard spectral simulation methods [11]. The interpretation is simpler than the EXAFS analysis, and the data provide details of the bonding symmetry that EXAFS cannot provide. Furthermore, the EFG can be calculated with high fidelity using a variety of quantum chemical techniques. We provide estimates of the magnitudes and symmetries of the Sb nuclear quadrupolar interaction. Since potential Sb bonding configurations must satisfy these values, our results serve as a guideline for obtaining reasonable models of these amorphous systems.

II. Experiment

A. Sample Preparation

All amorphous $Ge_2Sb_2Te_x$ (x = 4,5,7) samples were grown via the RF magnetron sputtering method. The sputtering targets consisted of crystalline $Ge_2Sb_2Te_x$ prepared according to Ref [12]. Depositions were made at room temperature with RF power level and argon gas pressure set to 51 Watt and 5 mTorr, respectively. The films were grown on commercially available aluminum foil, which were degreased by sonicating the foil in an isopropyl alcohol bath. The foil was then etched in a 3% HCl bath. The remaining Ge-Sb-Te flakes were rinsed with methanol, packed into a sample tube, and dried in air. The x-ray diffraction pattern of the flakes showed no evidence of the crystalline phase.

B. NMR Measurements

For these NMR experiments, we used a broadband spectrometer built in-house at the National High Magnetic Field Laboratory. The measurements were performed at 77 K, using a DC resistive magnet capable of producing 0 to 17.5 Tesla. The sample was placed in a hand-

wound coil made from 22 AWG solid copper wire. Typical coil Q values were approximately 150 at 77 K. The operating frequency was held constant at 178.32 MHz while the field was varied. At each field value, we employed a Carr-Purcell-Meiboom-Gill pulse sequence, which, due to the long spin-spin dephasing time for these materials, facilitated a tremendous improvement in the data acquisition time [10]. The signals for up to 50 spin echoes were collected, digitized, then co-added to yield the final signal, which was then analyzed. Typically, 10^3-10^5 traces were co-added to obtain a suitable signal-to-noise ratio for the time domain data. We determined the 90^o pulse lengths by maximizing the free induction decay signal of ^{63}Cu (due to the coil), and then scaling this number by the ratio of ^{63}Cu and ^{121}Sb magnetic moments. We took care to avoid the resonance field values for the stable ^{63}Cu and ^{65}Cu isotopes, which were easy to identify since they are very narrow compared to excitation bandwidth. The pulse spacing was typically 100 μsec and the time between successive applications of the pulse sequence was typically 50 msec.

C. Spectral Simulations

The theoretical fits to the ^{121}Sb NMR data we present were calculated using a powder averaging routine outlined in Ref [11]. Our calculations of the powder spectra use the nuclear Hamiltonian consisting of an applied magnetic field term and the complete nuclear quadrupole term:

$$\hat{H} = \gamma \vec{B} \vec{I}(\theta,\phi,\psi) + \frac{\nu_q}{40}[(3\hat{I}_z^2 - \hat{I}^2) + \eta(\hat{I}_x^2 - \hat{I}_y^2)], \qquad (1)$$

where γ (in MHz / Tesla) is the nuclear gyromagnetic ratio (γ = 10.18 MHz / Tesla for ^{121}Sb), B is the applied magnetic field, (θ,ϕ,ψ), are the Euler angles relating the orientation of B to the principle axes of the quadrupole interaction, $\hat{I}_i$ are the dimensionless spin operators, ν_q (in MHz) is the quadrupole coupling parameter, and η (dimensionless) is an asymmetry parameter which

can take the values $0 \leq \eta \leq 1$ [11]. This parameter signifies the symmetry of the field gradient tensor, which is intimately related to the bonding symmetry. In the case of eta = 0, the field gradient tensor is perfectly axially symmetric and suggests some manifestation of an axially symmetric bonding arrangement. In group V chalcogen binaries, such an arrangement is commonly observed when the quadrupole nucleus, in this case ^{121}Sb, is located at the apex of a pyramidal structure, bonded to three chalcogen atoms [6]. The parameter ν_q is related to the largest component of the electric field gradient tensor surrounding the quadrupolar nucleus.

In the simplest application of Eq. 1, the two free parameters, ν_q and η, are varied until the powder spectra converge on an acceptable representation of the experimental spectra. However, we find no one set of parameters generates a spectrum that accurately accounts for the broad features of our data. We therefore construct superposition of powder spectra using sets of ν_q and η, $\{\nu_q , \eta\}$ that are Gaussian distributed about an average value, denoted by "< >", with a full width at half maximum value (FWHM), denoted by "±". For example, the powder spectrum constructed from the set { <210> ± 100 , 0 } refers the superposition of powder spectra where the average ν_q = 210 MHz and FWHM of 100 MHz, with η = 0 for spectra. In cases where the FWHM value for η approaches 1, the parameter is undetermined, which has the physical interpretation that, on average, the bonding symmetry is completely disordered.

III. Results

The high field ^{121}Sb NMR experimental data (black squares) for the compositions of $Ge_2Sb_2Te_4$, $Ge_2Sb_2Te_5$, and $Ge_2Sb_2Te_7$ along with some representative simulations (dashed lines) are shown in Fig.1. Simulations of the full nuclear quadrupolar Hamiltonian, with no approximations to the quadrupole term, show that the peaks near 14.75 and 15.75 Tesla in Fig. 1 (b-c) arise from a substantial number of Sb sites having an approximately axially symmetric

bonding configuration. Moreover, the smoothly decaying intensity similar to the spectra of Fig. 1 (a) corresponds to a situation where there is little to no symmetry in the quadrupolar Hamiltonian. We find that components of the theoretical spectra for both axial and disordered sites are needed in order to capture all of the spectral features of Figs. 1 (b-c). The fitting parameters that produce the dashed lines in Fig. 1 are summarized in Table 1. The FWHM parameter measures the disorder of the structural unit. Thus, highly disordered sites have large FWHM values with respect to the average value. Additionally, the contribution of the axial Sb site to the total spectrum is also listed in Table 1.

Although the assumption of a Gaussian of ν_q and η needs refining, evidenced by the imperfect fits, these simulations do sufficiently replicate the spectral features essential for the structural interpretation. We find a progressive increase in the contribution of the axial Sb site as the tellurium content is increased. Qualitatively, these results are consistent with the same trend observed in the As_xS_{1-x} and As_xSe_{1-x} glasses, which are classic *8-N* systems [7] when x = 0.4. In the ideal analogy between the S and Se systems and the Te system, $Ge_2Sb_2Te_7$, which contains exactly enough Te to satisfy the valence requirements of Sb and Ge, should contain exclusively the ordered Sb site and only Ge-Te and Sb-Te bonds. However, the inclusion of approximately 45% of the disordered Sb site indicates that some bonding flaws occur, such as the appearance of homopolar or Ge-Sb bonds, as suggested from some structural models based on EXAFS data [13].

Great insight into the configuration of the axial Sb bonding unit is obtained by associating the measured coupling constants in Table 1 with those occurring in other As or Sb chalcogen compounds. The As_2X_3 and Sb_2X_3 systems, where X is a chalcogen atom (oxygen, sulfur, selenium, or tellurium), which are *8-N* systems, all contain an As (Sb) site wherein three

chalcogen atoms form a pyramid with the As (Sb) at the apex [6]. This configuration satisfies the axial bonding condition necessary to produce the types of spectra found for the axial Sb site in Table 1. In Fig. 2, we reproduce the measured values of ν_q from Ref [6] for those pyramidal sites with $\eta \sim 0$, normalized to those measured when the chalcogen atom is oxygen. Indeed, the scaling for X = oxygen, sulfur, and selenium is excellent confirmation of the equivalence of the pyramidal units when Sb is substituted for As. The overlap of the estimated coupling constant for the axial Sb site of $Ge_2Sb_2Te_5$ and $Ge_2Sb_2Te_7$ with that measured in As_2Te_3 strongly suggests that these axial Sb sites are analogous. Bobela and Taylor have shown that values of ν_q for the ^{121}Sb nucleus in the crystalline Ge-Sb-Te counterparts, where the Sb atoms take an octahedral bonding configuration, are approximately an order of magnitude smaller than those in the amorphous phase [14]. There is better agreement between these smaller values and those reported for higher coordinated Sb systems like MnSb or crystalline antimony Ref [15]. The spectrum for the crystalline phase of $Ge_2Sb_2Te_5$ does not possess the same fingerprint of an axial Sb site as seen in the spectrum of the amorphous phase. Although it is likely that vacancies influence the overall bonding symmetry of the Sb sites in the crystalline phase, the transition to the pyramidal sites in the amorphous phase involves a non-intuitive transition from a disordered octahedral site to two three-fold, pyramidal sites, one of which is more well-defined.

It is more difficult to assess a structural analogy for the disordered Sb site. In Sb_2S_3 and Sb_2Se_3 a second pyramidal bonding configuration exists whereby the Sb atom has two nearby, but non-bonded, chalcogen atoms above the apex of the pyramidal unit. The proximity of nearby chalcogen atoms complicates the symmetry of the electric field gradient at the nucleus and raises the value of η from ~ 0 to ~ 0.7 [6]. These sites produce coupling constants similar to those measured for the disordered sites in this work. Thus the large variation in η for the disordered

sites may be due to the proximity of other chalcogens, which is a consequence of system's departure from the ideal *8-n* composition, $Ge_2Sb_2Te_7$.

With respect to structural models of the amorphous phase, the NMR data presented in Table 1 provide an essential experimental result that must be fulfilled by theory. We have shown that the configurations responsible for the estimated coupling constants and asymmetry parameters of the amorphous phase are a manifestation of a 3-fold, pyramidal Sb site. We therefore suggest that subsequent structural modeling of the amorphous phase begins with these types of sites as building blocks. Calculations of the field gradients, however, especially for heavy elements such as Sb, are far from trivial owing to the increasing importance of spin-orbit effects. To the best of our knowledge, there are no published, successful theoretical calculations of coupling constants for ^{121}Sb in Ge-Sb-Te compounds and very few studies concerning related materials (see for instance reference [15] and references therein). Recently, the combination of cluster calculations with periodic calculations for model amorphous systems has been used to show that standard exchange correlation potentials, such as LDA and PBE, systematically underestimate electric field gradients for S, Se, and Sb [16], due the absence of exact exchange, and are, thus, inappropriate for delineating local structures. Pure Hartree-Fock theory over estimates the electric field gradient. However, inclusion of exact exchange, as in the hybrid exchange correlation potential B3LYP, led to significantly better agreement with experiment for all three chalcogens. Cluster calculations using B3LYP do reproduce the present results provided that the three-fold coordinated Sb in the amorphous phase is bonded exclusively to two-fold coordinated Te in the axial site and to one or two three-fold coordinated Te for the anisotropic site [16]. There is often justifiable concern about using finite clusters to simulate sites in infinite systems. We should point out that calculations of EFG on finite clusters abstracted from periodic

super cells of GST compounds at both the LDA and PBE levels of approximation were in excellent agreement with the purely periodic results at the same level of approximation, indicating that for these highly covalent systems, cluster calculations are a very reliable tool.

Acknowledgements

The authors gratefully acknowledge support from the Air Force Office of Scientific Research under grant number FA9453-07-1-0202 and the National Science Foundation under grant number DMR 0702351.

References

1. S. R. Ovshinsky, *Phys. Rev. Lett.* **21**, 1450–1453 (1968)
2. A. V. Kolobov, *et al*. *Nature Mater.* **4**, 703–708
3. D. A. Baker, *et al*. *Phys. Rev. Lett.* **96**, 255501 (2006).
4. P. Jovari, *et al. Phys. Rev. B* **77**, 035202 (2008).
5. J. Hegedüs, S. R. Elliott, *Nature Mater.* **7**, 399–405 (2008).
6. T. Das, E. Hahn, *Nuclear Quadrupole Resonance Spectroscopy* (Academic Press, New York, 1958).
7. T. Su, *et al. Phys. Rev. B.* **67**, 085203 (2003).
8. E. Mammadov, P. C. Taylor, *J. Non-Cryst. Sols.* **354** (2008).
9. D. C. Bobela, P. C. Taylor, *J. of Non-Cryst. Sols*. **354** (2008).
10. A. Abragam, *Principles of Nuclear Magnetism* (Oxford University Press, New York, 1994).
11. M. Edén, *Conc. in Mag. Res. A*. **17A,** 117 (2003).
12. J. K. Olson *et al.*, *J. Appl. Phys*. **99**, 103508 (2006).
13. M. A. Paesler, D. A. Baker, G. J. Lucovsky, *Non-Crsyt. Sols*. **354**, 2706-2710 (2008).
14. D. C. Bobela, P. C. Taylor, *Mater. Res. Soc. Symp. Proc.* **1072**, (2008).
15. A. Svane, *Phys. Rev. B.* **68,** 064422 (2003).
16. A. Edwards, *private comms.* (2008).

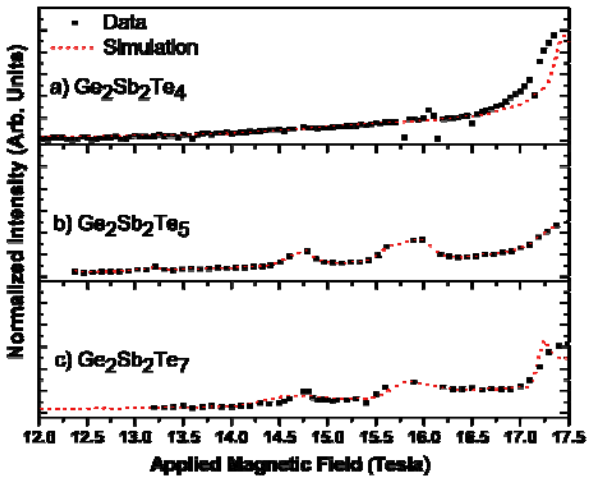

FIG 1. High field ^{121}Sb NMR data in the amorphous compounds a) $Ge_2Sb_2Te_4$, b) $Ge_2Sb_2Te_5$, and c) $Ge_2Sb_2Te_7$. Dashed lines are representations of best-fit simulated spectra. The smoothly decaying signal in a) indicates an Sb site with low bonding symmetry while the emergence of peaks near 14.75 Tesla and 15.75 Tesla in b) and c) demonstrates the existence of a nearly axially symmetric bonding configuration around the Sb atom.

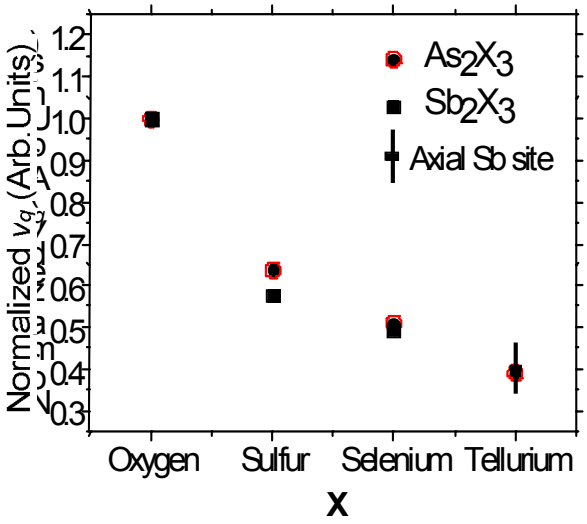

FIG. 2. Coupling constants, ν_q, for ^{75}As and ^{121}Sb nuclei in As_2X_3 and Sb_2X_3 compounds where X is a chalcogen atom. Values have been normalized to the coupling constant when X = oxygen. In these compounds the As and Sb nuclei form 3-fold, pyramidal structures with the As or Sb at the apex. The overlap in the estimated coupling constant of the axial Sb site suggests that these sites are configured similar to the binary compounds.

TABLE I: Summary of simulation parameters of the best-fit lines in Fig. 1 using a Gaussian distribution with an average and FWHM denoted by < > ± FWHM. The average coupling constant and asymmetry parameter is indicated by $<\nu_q>$ and $<\eta>$, respectively. The fraction of the axial Sb site used in the total spectrum is also shown. These data are the direct consequence of the Sb bonding environment and therefore represent a useful guide for structural modeling of the amorphous Ge-Sb-Te compounds.

Composition	Disordered Sb		Axial Site		% Axial Sb
	$<\nu_q>$ (MHz)	$<\eta>$	$<\nu_q>$ (MHz)	$<\eta>$	
$Ge_2Sb_2Te_4$	210 ± 100	0.75 ± 0.1	--	--	0
$Ge_2Sb_2Te_5$	360 ± 120	0.75 ± 0.1	220 ± 40	0 ± 1	25
$Ge_2Sb_2Te_7$	360 ± 120	0.75 ± 0.1	220 ± 40	0 ± 1	55